Journal of Biomolecular NMR, **15:** 27–37, 1999.
KLUWER/ESCOM

Quantitative estimation of magnitude and orientation of the CSA tensor from field dependence of longitudinal NMR relaxation rates

Peter Damberg[a], Jüri Jarvet[a], Peter Allard[b] & Astrid Gräslund[a,*]
[a]*Department of Biophysics, Arrhenius Laboratories, Stockholm University, S-106 91 Stockholm, Sweden;* [b]*Center for Structural Biochemistry, Department of Biotechnology, The Royal Institute of Technology, NOVUM, S-141 57 Huddinge, Sweden*

Received 24 March 1999; Accepted 14 June 1999

Key words: cross-correlation, CSA, NMR relaxation, tyrosine

Abstract

A method is presented that makes it possible to estimate both the orientation and the magnitude of the chemical shift anisotropy (CSA) tensor in molecules with a pair of spin 1/2 nuclei, typically ^{13}C-^{1}H or ^{15}N-^{1}H. The method relies on the fact that the longitudinal cross-correlation rate as well as a linear combination of the autorelaxation rates of longitudinal heterospin magnetization, longitudinal two-spin order and longitudinal proton magnetization are proportional to the spectral density at the Larmor frequency of the heterospin. Therefore the ratio between the cross-correlation rate and the above linear combination is independent of the dynamics. From the field dependence of the ratio both the magnitude and the orientation of the CSA tensor can be estimated. The method is applicable to molecules in all motional regimes and is not limited to molecules in extreme narrowing or slow tumbling, nor is it sensitive to chemical exchange broadening. It is tested on the 22 amino acid residue peptide motilin, selectively ^{13}C labeled in the ortho positions in the ring of the single tyrosine residue. In the approximation of an axially symmetric ^{13}C CSA tensor, the symmetry axis of the CSA tensor makes an angle of $23° \pm 1°$ to the ^{13}C-^{1}H bond vector, and has a magnitude of 156 ± 5 ppm. This is in close agreement with solid-state NMR data on tyrosine powder [Frydman et al. (1992) *Isr. J. Chem.*, **32**, 161–164].

Introduction

Knowledge about the parameters characterising the chemical shift anisotropy (CSA) is necessary when NMR relaxation rates are used to study the dynamics of molecules. This is particularly important when experiments are performed at high magnetic fields. The CSA of α-carbons in proteins has also been shown to correlate with secondary structure (Tjandra and Bax, 1997a) and the CSA of amide nitrogens and attached protons correlates with hydrogen bond length (Tjandra and Bax, 1997b).

Recently attempts have been made to estimate the average magnitude of the CSA and the orientation from standard relaxation data sets (T_1, T_2 and NOE) (Boyd and Redfield, 1998). Another branch of experiments aiming at the CSA comes from studies of weakly aligned proteins (Ottiger et al., 1997). A common method has been to estimate the CSA from the interference effect between the CSA and dipole–dipole (DD) relaxation mechanisms. However, this approach suffers from not being able to separate the effects of orientation and magnitude of the CSA (Tessari et al., 1997a,b; Tjandra and Bax, 1997a,b; Fushman and Cowburn, 1998).

Very recently Fushman and co-workers (Fushman et al., 1998b) reported a method to estimate both the magnitude and the orientation of the CSA parameters from field-dependent ratios between the transverse relaxation rate and the transverse cross-correlation rate. Here we present a method in the same spirit, where the field dependence of three longitudinal autorelaxation rates and the longitudinal cross-correlation rate are

*To whom correspondence should be addressed. E-mail: astrid@biophys.su.se

used. Thereby one avoids the possible problems associated with conformational exchange contributions to the autorelaxation and the approximation concerning the high frequency components of the spectral density function. The presented method is the first one that is applicable in all motional regimes, i.e. also for rapidly rotating molecules and flexible parts of larger molecules like the side chains in proteins. This also opens up the possibility of comparing the CSA of small model compounds studied by solid-state NMR with the CSA obtained from relaxation studies in solution. It is straightforward to apply the same method to measure the CSA parameters also of uniformly ^{15}N labeled peptides and proteins. Deuteration will help to increase the accuracy of measured rates by minimising the relaxation caused by surrounding protons. Uniformly ^{13}C labeled proteins will have contributions from ^{13}C-^{13}C interactions and therefore will require a different approach to measure and to evaluate the CSA parameters.

We have applied the longitudinal relaxation rate method to evaluate the CSA parameters of a CH bond in the aromatic ring of tyrosine in a peptide hormone and compared the results to literature data on tyrosine powder studied by solid-state NMR (Frydman et al., 1992).

Theory

The interference between the CSA and dipole–dipole relaxation mechanisms, i.e. cross-correlation, can be observed as a conversion between longitudinal magnetization and two-spin order. For an axially symmetric ^{13}C CSA tensor the rate of conversion (cross-correlation rate δ_C) could be expressed as (Goldman, 1984):

$$\delta_C = -\frac{\mu_0}{4\pi}\frac{\hbar\gamma_H\gamma_C^2}{r_{CH}^3}\Delta\sigma B_0 P_2(\cos(\beta))\cdot J(\omega_C) \quad (1)$$

Here $\Delta\sigma = \sigma_{||} - \sigma_\perp$ is the difference between the shielding of the nucleus under study when the static field is parallel, $\sigma_{||}$, and orthogonal, $\sigma_\perp$, to the symmetry axis of the CSA tensor. B_0 is the static magnetic field, γ_C and γ_H are the gyromagnetic ratios of ^{13}C and proton, respectively, μ_0 is the permeability of vacuum and $\hbar$ is Plank's constant. P_2 symbolizes the second Legendre polynomial, $P_2(\cos(\beta)) = (3\cos^2(\beta)-1)/2$, where β is the angle between the internuclear vector and the symmetry axis of the CSA tensor, r_{CH} is the carbon-proton distance. $J(\omega_C)$ is the spectral density at the Larmor frequency of the carbon, where the spectral density function is normalized so that its integral from $-\infty$ to ∞ equals $2\pi/5$. This implies that for e.g. isotropic Brownian motion $J(\omega) = (2/5)\tau_C/(1+(\tau_C\omega)^2)$

The spectral density $J(\omega_C)$ can be calculated from the auto-relaxation rates of longitudinal carbon magnetization, ρ_C, longitudinal two-spin order, ρ_{CH}, and longitudinal proton magnetization, ρ_H (Peng and Wagner, 1992):

$$J(\omega_C) = \frac{\rho_C + \rho_{CH} - \rho_H}{2\left(\frac{1}{3}\Delta\sigma^2 B_0^2\gamma_C^2 + 3\left(\frac{\mu_0}{4\pi}\right)^2\frac{\hbar^2\gamma_H^2\gamma_C^2}{4r_{CH}^6}\right)} \quad (2)$$

When Equations 1 and 2 are combined and rearranged:

$$\begin{aligned} B_0\frac{\rho_C + \rho_{CH} - \rho_H}{\delta_C} &= \frac{4\pi}{\mu_0}\frac{-2\Delta\sigma r_{CH}^3}{3\hbar\gamma_H P_2(\cos(\beta))}\cdot B_0^2 \\ &\quad -\frac{\mu_0}{4\pi}\frac{3\hbar\gamma_H}{2\Delta\sigma r_{CH}^3 P_2(\cos(\beta))} \\ &= slope\cdot B_0^2 + intercept \quad (3) \end{aligned}$$

From a field-dependent relaxation study of longitudinal relaxation and cross-correlation one can obtain the slope and intercept parameters in Equation 3. The magnitude of the CSA can be calculated as:

$$|\Delta\sigma| = \sqrt{\frac{slope}{intercept}}\cdot\frac{3\hbar\gamma_H\mu_0}{8\pi r_{CH}^3} \quad (4)$$

and the orientation factor:

$$|f_{orient}| = |P_2(\cos(\beta))| = (slope\cdot intercept)^{-1/2} \quad (5)$$

The signs of $P_2(\cos(\beta))$ and $\Delta\sigma$ are somewhat ambiguous, but their relative signs can be backtraced from the sign of the cross-correlation rate. If the cross-correlation rate is positive, then either $P_2(\cos(\beta))$ or $\Delta\sigma$ is negative. If the cross-correlation rate is negative they both have the same sign. If $|P_2(\cos(\beta))| > 0.5$, as determined from experimental data using Equation 5, then $P_2(\cos(\beta))$ is positive and the sign of $\Delta\sigma$ follows from the sign of the cross-correlation rate, while if $|P_2(\cos(\beta))| < 0.5$ only the relative signs of $P_2(\cos(\beta))$ and $\Delta\sigma$ and their absolute numerical values can be determined.

For the general case, when the CSA tensor is not axially symmetric, a relaxation effective magnitude is

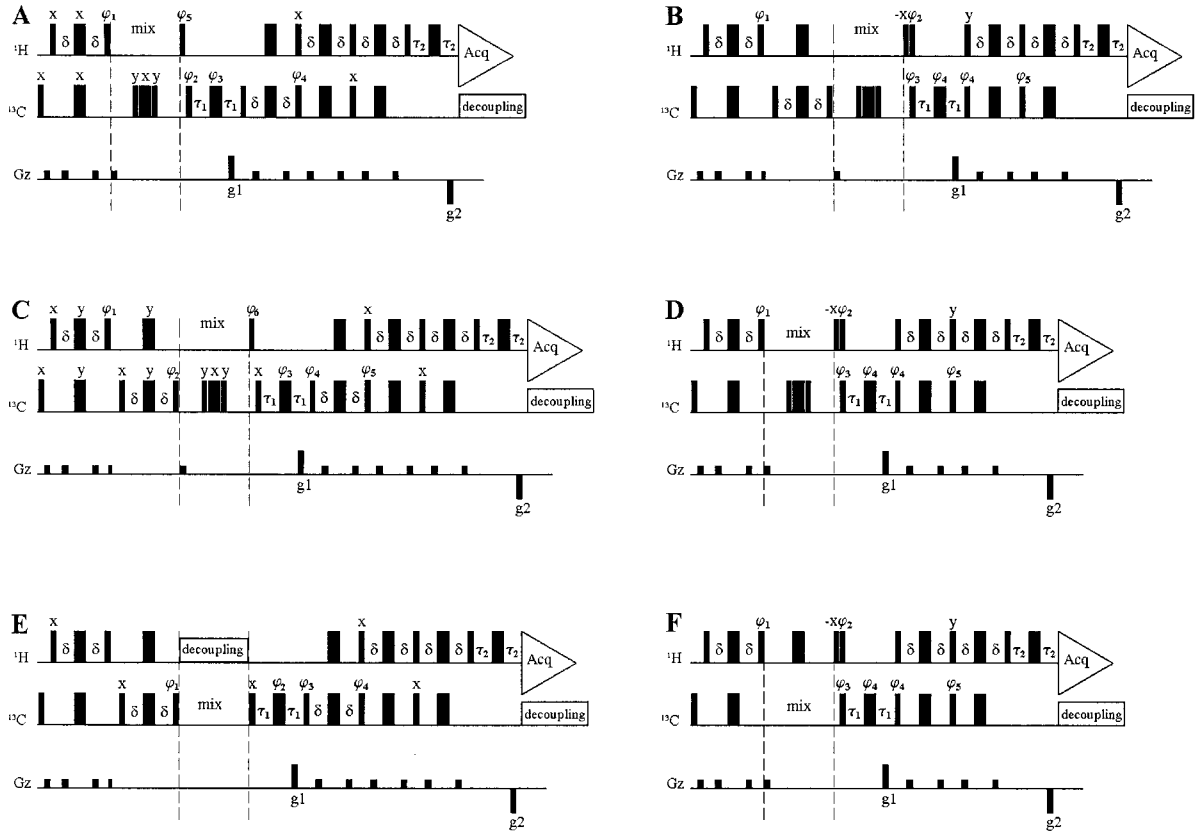

Figure 1. The heteronuclear pulse sequences with sensitivity enhancement used for measuring the relaxation parameters discussed in the text. Black thin and thick vertical bars represent 90° and 180° pulses, respectively. (A) Pulse sequence for following the buildup of carbon magnetization from two-spin order. The phase is y when nothing else is stated. φ_1 = 4(y), 4(−y); φ_2 = x, −x; φ_3 = 2(x), 2(−x); φ_4 = 2(y), 2(−y); φ_5 = 8(x), 8(−x); Acq. = x, −x, −x, x, −x, x, x, −x; (B) Pulse sequence for following the buildup of two-spin order from carbon magnetization. φ_1 = 4(y), 4(−y); φ_2 = 8(x), 8(−x); φ_3 =y, −y; φ_4 = 2(x), 2(−x); φ_5 = 2(y), 2(−y); Acq. = x, −x, −x, x, −x, x, x, −x, −x, x, x, −x, x, −x, −x, x; (C) Pulse sequence for following the decay of carbon magnetization when cross-correlation is active. φ_1 = 4(y), 4(−y); φ_2 =y, −y; φ_3 = 2(x), 2(−x); φ_4 = y, φ_5 = 2 (y); 2(−y); φ_6 = 8(x), 8(−x); Acq. = x, −x, −x, x, −x, x, x, −x; (D) Pulse sequence for following the decay of two-spin order when cross-correlation is active. The phase is y when nothing else is stated. φ_1 = 4(y), 4(−y); φ_2 = 8(x), 8(−x); φ_3 =x, −x; φ_4 = 2(x), 2(−x); φ_5 = 2(y), 2(−y); Acq. −= x, −x, −x, x, −x, x, x, −x, −x, x, x, −x, x, −x, −x, x; (E) Pulse sequence for measuring the autorelaxation rate of longitudinal carbon magnetization, when cross-correlation is suppressed so as to obtain a single exponential decay. The phase is y when nothing else is stated. φ_1 =y, −y; φ_2 = 2(x), 2(−x); φ_3 =y; φ_4 = 2(y), 2(−y); Acq. = x, −x, −x, x; (F) Pulse sequence for measuring the autorelaxation rate of two-spin order, when cross-correlation is suppressed so as to obtain a single exponential decay. The phase is x when nothing else is stated. φ_1 = 8(y), 8(−y); φ_2 = 4(x), 4(−x); φ_3 = x, −x; φ_4 = 2(x), 2(−x); φ_5 = 2(y); Acq. = x, −x, −x, x, −x, x, x, −x, −x, x, x, −x, x, −x, −x, x.

obtained in Equation 4 together with an orientation factor in Equation 5. The effective CSA is:

$$\Delta\sigma_{eff} = \sqrt{\sigma_{xx}^2 + \sigma_{yy}^2 + \sigma_{zz}^2 - (\sigma_{xx}\sigma_{yy} + \sigma_{xx}\sigma_{zz} + \sigma_{yy}\sigma_{zz})} \quad (6)$$

where σ_{xx}, σ_{yy} and σ_{zz} are the principal values of the CSA tensor.

The expression for the cross-correlation rate of an asymmetric CSA tensor was derived as outlined by Canet (1998), and is as follows:

$$\delta_C = -\frac{\mu_0}{4\pi}\frac{\hbar\gamma_C^2\gamma_H}{r_{CH}^3}B_0 \cdot \left[(\sigma_{zz} - \sigma_{yy})\frac{3\cos^2\theta_{z,r} - 1}{2} + (\sigma_{xx} - \sigma_{yy})\frac{3\cos^2\theta_{x,r} - 1}{2}\right] \cdot J(\omega_C) \quad (7)$$

Since the expression between the square brackets, related to the projection of the CSA tensor on the CH

bond vector, is constant, it can always be expressed as a proportionality constant f_{orient}. multiplied by the effective CSA, $\Delta\sigma_{eff}$:

$$(\sigma_{zz} - \sigma_{yy})\frac{3\cos^2\theta_{z,r} - 1}{2} + (\sigma_{xx} - \sigma_{yy})\frac{3\cos^2\theta_{x,r} - 1}{2} \equiv f_{orient} \cdot \Delta\sigma_{eff} \quad (8)$$

where $\theta_{z,r}$ is the angle between the z principal axes of the CSA tensor and the CH bond vector and $\theta_{x,r}$ is the angle between the x principal axes of the CSA tensor and the CH bond vector.

With these definitions $\Delta\sigma_{eff}$ is always positive (see Equation 6), while f_{orient} can take any value between -1 and 1. This is somewhat different from the standard convention where $\Delta\sigma$ is defined as the shielding when the main field is parallel, $\sigma_{||}$, to the symmetry axis of the shielding tensor minus the shielding when the main field is orthogonal, $\sigma_{\perp}$, to the symmetry axis. With this convention $\Delta\sigma$ can be either positive or negative, while the term $P_2(\cos(\beta))$, related to the orientation of the CSA tensor in the molecular frame, can take any value between $-1/2$ and 1.

For a cylindrically symmetric CSA tensor, if $\sigma_{||} > \sigma_{\perp}$, then $f_{orient} = P_2(\cos(\beta))$ and $\Delta\sigma_{eff} = \Delta\sigma = \sigma_{||} - \sigma_{\perp}$, whereas if $\sigma_{||} < \sigma_{\perp}$ the $f_{orient} = -P_2(\cos(\beta))$ and $\Delta\sigma_{eff} = -\Delta\sigma = -(\sigma_{||} - \sigma_{\perp})$.

Experimental

Sample

The method for obtaining information concerning the CSA tensor from relaxation experiments in liquids outlined above was tested on a peptide sample containing motilin with 22 amino acid residues and labeled with ^{13}C in the ortho positions of the aromatic ring of the single tyrosine residue. The concentration of the peptide was 5 mM in 30% hexafluoroisopropanol-d/10% D_2O/60% H_2O. The peptide was manually synthesised using stepwise *tert*-butyloxycarbonyl (t-Boc) solid phase synthesis as previously described (Allard et al., 1995). The ^{13}C labeled tyrosine was purchased from Cambridge Isotope Laboratories. A t-Boc protecting group was attached according to prescribed procedures. The purity was checked with analytical HPLC (C_{18} column 218TP1010, Vydac). The correct molecular mass, 2699.5 Da, was confirmed by an experimental mass determined to be 2697.8 Da, using plasma desorption mass spectrometry (Model Bioion 20, Applied Biosystems).

NMR spectroscopy

Experiments were performed using Varian Inova spectrometers operating at 18.79, 14.09 and 9.39 T corresponding to proton resonance frequencies of 800, 600 and 400 MHz, respectively. A recycle delay of 5 s was used, including 1.5 s low power water saturation and the acquisition time. All experiments were carried out at 318 K. Hard proton and carbon pulse widths were about 7 and 18 μs, respectively, on all spectrometers. The proton frequency was placed approximately 50 Hz off-resonance. The carbon frequency was set on-resonance. Carbon decoupling was achieved by continuous wave decoupling with a B_1 field of ca. 0.5 kHz.

Pulse sequences

The pulse sequences for measuring cross-correlation are shown in Figure 1A–D. The rate of conversion between longitudinal carbon magnetization (Cz) and two-spin order (2HzCz), i.e. the cross-correlation rate, was measured by following either the carbon magnetization (Figure 1A,C), or the two-spin order (Figure 1B,D), after either an inversion of the carbon magnetization (Figure 1B,C) or preparation of two-spin order (Figure 1A,D), in four separate experiments.

The pulse sequences were developed from the pulse sequences of Dayie and Wagner (1994) and use proton excitation and detection of transient magnetization and pulse field gradients for coherence selection and water suppression.

A carbon inversion pulse was inserted in the middle of the mixing time (Figure 1A–D) for suppression of unwanted relaxation pathways (mainly heteronuclear cross-relaxation). This makes it possible to fit the cross-correlation rate without having to consider the heteronuclear cross-relaxation rate and the autorelaxation rate of the proton. Furthermore, the phase cycles were adjusted so as to obtain a decay towards zero intensity in the inversion recovery type of experiments (Freeman and Hill, 1971).

The proton pulse(s) immediately after the mixing time were found necessary for suppressing a dispersive artifact at short mixing times in the buildup experiments.

In two separate experiments the pulsing during the mixing time was changed so as to obtain single exponential decays of longitudinal carbon magnetization (Figure 1E) and longitudinal two-spin order

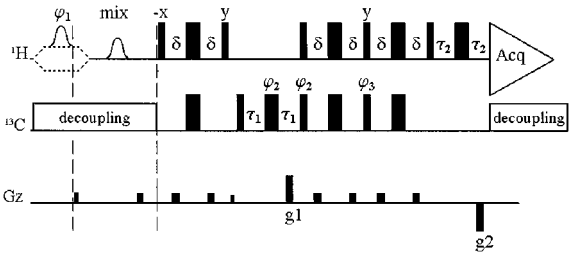

Figure 2. Pulse sequence for measuring the autorelaxation rate of longitudinal proton magnetisation. φ_1 = 4(x), 4(−x); φ_2 = 2(x), 2(−x); φ_3 = 2(y), 2(−y); Acq. = x, −x, x; the phase is x when nothing else is stated. Selective proton inversion pulses are indicated with bell-shaped symbols.

(Figure 1F). This was achieved by broadband proton decoupling for longitudinal carbon magnetization and by a proton inversion in the middle of the mixing time for two-spin order, which effectively suppresses the CSA-DD cross-correlation effect (Boyd et al., 1990; Kay et al., 1992; Palmer et al., 1992). By using the extended phase cycle instead of the original pulse sequence (Dayie and Wagner, 1994) to average the relaxation of positive and negative two-spin order, the potential cross-relaxation with other protons becomes effectively indirect.

The autorelaxation rate of longitudinal proton magnetization was measured using the pulse sequence of Figure 2. The experiments were performed in accordance with the suggestions by Norwood (1996, 1997), in an add/subtract manner, with selective proton inversion in the middle of the relaxation delay, to obtain a single exponential decay towards zero.

For all pulse sequences (Figure 1A–F and Figure 2) the delay δ was set to $(4J)^{-1}$ where J is the one-bond scalar coupling constant of 159 Hz. Before each pulse sequence, 1.5 s low power water saturation was used. The delays $\tau 1$ and $\tau 2$ were set to 0.7075 ms and 0.4257 ms, respectively.

Experiments at (800, 600, 400 MHz): An acquisition time of (512, 512,128 ms) was used. The gradient pulses g1 and g2 were applied with strengths of ca. (0.6, 0.3, 0.6) T/m during 0.61 and 0.15 ms, respectively. The precise strength of the g2 pulse was adjusted to meet the criterion $g1 \cdot t1/g2 \cdot t2 = \gamma_H/\gamma_C$.

In the experiments where cross-correlation was effective (sequences in Figure 1A, B, C and D) (64, 64, 288) transients were added for each mixing time. (16, 16, 12) different mixing times between (1, 1, 5) ms and (1.4, 1.7, 1.4) s were sampled, more densely for shorter mixing times.

In the experiments for measuring the autorelaxation rate of carbon magnetization, ρ_C (pulse sequence in Figure 1E) and in the experiment for measuring the autorelaxation rate of two-spin order, ρ_{CH} (pulse sequence in Figure 1F), (64, 16, 128) transients were added for each of the (30, 30, 14) mixing times between (1, 1, 5) ms and (640, 640, 300) ms.

In the proton autorelaxation experiment (16, 48, 128) transients were added and (24, 27, 14) different mixing times between (5, 5, 3) ms and (0.9, 0.9, 0.77) s were sampled. A recycling time of (8, 6, 3.1) s was used. For selective proton inversion (53.5, 42.5, −) ms Isnob2 pulses (Kupče et al., 1995) were used. BIRD pulses (Garbow et al., 1982) were used for selective proton inversions at 400 MHz, since the difference in resonance frequency between the protons at positions 2 and 6 in the ring and the protons attached to the labeled carbons was considered small.

Results

The experimental magnetization decay and buildup curves from experiments at 400 MHz (9.39 T) are shown in Figure 3 together with the fitted curves. The decay and buildup curves when cross-correlation is effective and other cross-relaxation pathways are suppressed can be described by two coupled differential equations (Felli et al., 1998):

$$\frac{\mathrm{d}}{\mathrm{dt}}\begin{pmatrix}\Delta\langle C_z\rangle\\ \Delta\langle 2H_zC_z\rangle\end{pmatrix} = -\begin{pmatrix}\rho_C & \delta_C\\ \delta_C & \rho_{CH}\end{pmatrix}\cdot\begin{pmatrix}\Delta\langle C_z\rangle\\ \Delta\langle 2H_zC_z\rangle\end{pmatrix} = -\mathbf{R}\cdot\Delta\mathbf{M} \qquad (9)$$

with the solution (Najfeld et al., 1996)

$$\Delta\mathbf{M}(t) = \exp(-t\mathbf{R})\cdot\Delta\mathbf{M}(0) \qquad (10)$$

With the initial conditions $\Delta\langle C_z\rangle(0) = C_z^0$ and $\Delta\langle 2H_zC_z\rangle(0) = 0$, the solution to Equation 9 will describe the decay of carbon magnetisation, $c_{de} \cdot \Delta\langle C_z\rangle(t)$, when cross-correlation is effective. Here c_{de} is a constant slightly less than unity, describing the slightly less efficient detection of carbon magnetization compared to two-spin order due to a longer pulse sequence. With the initial conditions $\Delta\langle C_z\rangle(0) = 0$ and $\Delta\langle 2H_zC_z\rangle(0) = 2H_zC_z^0$, the solution to Equation 9 will describe the buildup of carbon magnetisation, $c_{de} \cdot \Delta\langle C_z\rangle(t)$, from two-spin order. With the

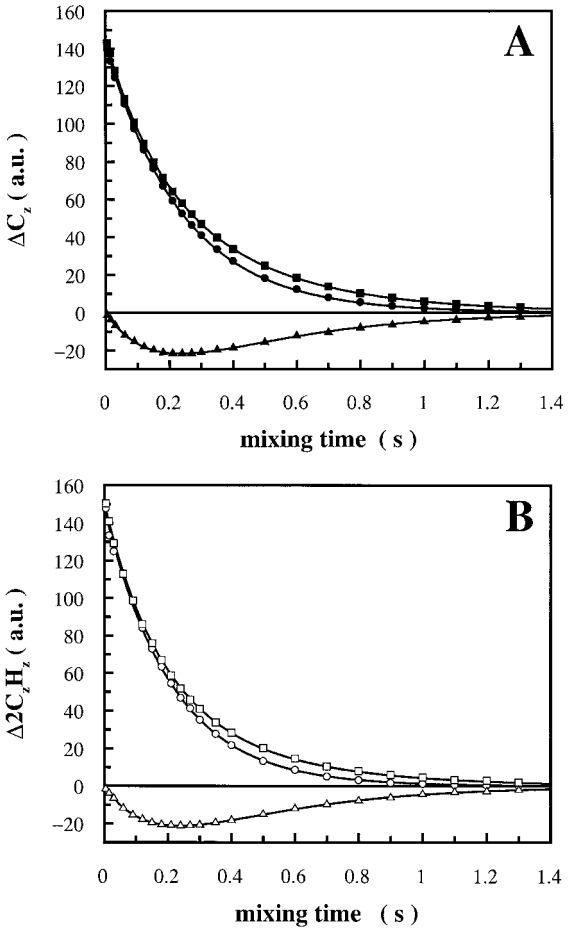

Figure 3. The experimental data set from the lowest field (9.39 T) with the lowest accuracy. The experimental intensities are shown together with their fitted curves, as solutions to Equation 9, described in the text. (A) shows the time evolution of carbon magnetization. The filled triangles are the experimental results from the experiment when two-spin order was created and carbon magnetization was detected (the sequence of Figure 1A). The filled squares are the experimental results from the decay experiment when cross-correlation was active (the sequence of Figure 1C). The filled circles are the experimental results when care was taken to achieve a single exponential decay (the sequence of Figure 1E). (B) shows the time evolution of two-spin order. Open triangles represent the buildup from longitudinal carbon magnetization and were obtained by using the sequence of Figure 1B. The open squares are the decay of two-spin order when cross-correlation was active, obtained by the pulse sequence of Figure 1D. The open circles are the decay of two-spin order when care was taken to suppress cross-correlation to achieve a single exponential decay obtained by the sequence of Figure 1F.

Table 1. Relaxation rates (s^{-1}) measured at 35 °C and at three magnetic fields for the ortho carbons of tyrosine in motilin. The uncertainties refer to one standard deviation confidence limit, estimated by the fitting procedure

	9.39 T (400 MHz)	14.09 T (600 MHz)	18.79 T (800 MHz)
ρ_C	4.15 ± 0.02	3.05 ± 0.01	2.58 ± 0.01
ρ_{CH}	4.78 ± 0.02	3.98 ± 0.02	3.45 ± 0.01
ρ_H	2.81 ± 0.03	2.08 ± 0.01	1.60 ± 0.01
δ_C	1.72 ± 0.02	1.69 ± 0.01	1.62 ± 0.01

initial conditions $\Delta\langle C_z\rangle(0) = 0$ and $\Delta\langle 2H_zC_z\rangle(0) = 2H_zC_z^0$, the solution to Equation 9 will describe the decay of two-spin order, $\Delta\langle 2H_zC_z\rangle(t)$, when cross-correlation is effective. With the initial conditions $\Delta\langle C_z\rangle(0) = C_z^0$ and $\Delta\langle 2H_zC_z\rangle(0) = 0$ the solution to Equation 9 will describe the buildup of two-spin order, $\Delta\langle 2H_zC_z\rangle(t)$, from carbon magnetisation.

The equations

$$I_C(t) = I_C^0 \exp(-\rho_C t) \tag{11}$$

and

$$I_{CH}(t) = I_{CH}^0 \exp(-\rho_{CH} t) \tag{12}$$

were used to fit to the experimental data when care was taken to suppress cross-correlation. All eight parameters ρ_C, ρ_{CH}, δ_C, C_z^0, $2H_zC_z^0$, I_C^0, I_{CH}^0 and c_{de} were fitted to all six experimental data sets in a simultaneous fit, using the Levenberg–Marquardt algorithm in the program gnuplot v. 3.6. The obtained relaxation rates ρ_C, ρ_{CH}, and δ_C are summarized in Table 1. The decay curves from the proton autorelaxation experiments were adequately fitted by a two-parameter single exponential decay curve and the rates (ρ_H) are shown in Table 1.

As described in the Theory section, a linear curve should be obtained when $B_0(\rho_C + \rho_{CH} + \rho_H)/\delta_C$ is plotted as a function of the magnetic field squared. The experimental data and the fitted line are shown together in Figure 4.

The effective magnitude of the CSA was calculated according to Equation 4. The relaxation effective CSA was estimated to be 153±5 ppm when the numerical value of $r_{CH} = 1.09$ Å was used. The orientation factor was estimated to be -0.76 ± 0.02 using Equation 5. The obtained results are shown in Table 2, where they are compared to the results of the solid-state NMR experiments of Frydman et al. (1992) on tyrosine powder. The uncertainties of the σ_{eff} and

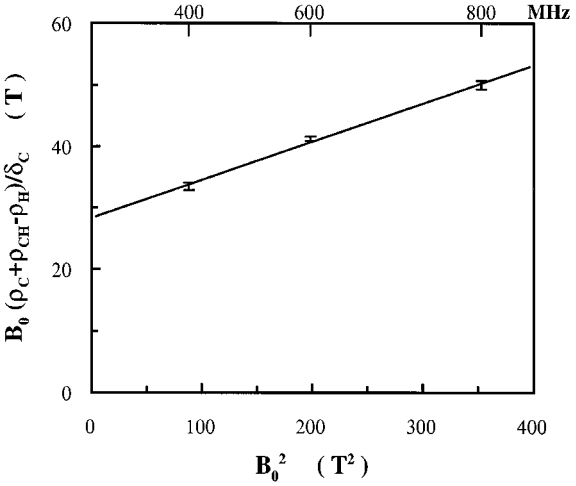

Figure 4. The ratio between the linear combination of the autorelaxation rates proportional to $J(\omega_C)$ and the cross-correlation rate, times the magnetic field as a function of the magnetic field squared, together with the least-squares fitted line corresponding to: $B_0 \frac{\rho_C+\rho_{CH}-\rho_H}{\delta_{CCH}} = (0.062 \pm 0.004)T^{-1} \cdot B_0^2 + (28.29 \pm 0.85)T$.

f_{orient} parameters were obtained from Monte Carlo simulations using 3000 randomly distributed synthetic data sets as described by Palmer et al. (1991). Standard errors of relaxation rates were obtained by the fitting procedure.

Since the solid-state experiment used by Frydman does not give any information concerning the orientation of the principal axis of the CSA tensor, we conducted an ab initio calculation using Gaussian98 for obtaining the orientation of the principal axes in the molecular frame, using *p*-cresol as a model compound. The structure was geometry optimized using the B3LYP method and a 6-31G(d) basis set, and showed a certain asymmetry of the hydroxyl group in the aromatic plane. For the NMR parameter calculation the Hartree–Fock method was used with the 6-311+G(2d,p) basis set and the optimized coordinates. The results for the two non-equivalent ortho carbons are shown in Table 2. This calculation allowed us to fix the principal axes in the molecular frame also for the solid-state NMR results. The least shielded component is parallel to the CH bond, the most shielded component is orthogonal to the plane of the aromatic ring and the intermediate component is orthogonal to the other two.

Discussion

In this work we have shown a precise and robust method for measurement of the CSA for a pair of spin 1/2 nuclei. The data allows independent estimations of the magnitude and the orientation of the CSA. A reliable estimation of the CSA parameters and their variations depending on the molecular environment is needed for interpretation of NMR relaxation experiments in terms of molecular dynamics. The values found here for the ortho carbons of tyrosine in a short peptide are in good agreement with solid state data on tyrosine powder (Frydman et al., 1992). The orientation factor f_{orient} describes the angle between the symmetry axis of a cylindrically symmetric CSA tensor and the internuclear vector and takes the value 1 when they are collinear. It should be noticed that this factor determines the theoretical limit of the resolution improvement in the TROSY experiment (Pervushin et al., 1997), since it determines the degree by which dipole–dipole and CSA relaxation can attenuate one another (optimal attenuation is obtained for collinear vectors).

Systematic errors may influence the determination of the CSA parameters. We have particularly considered two potential sources of errors: (1) anisotropic motions, and (2) additional relaxation by neighboring protons.

(1) Anisotropic motions could in principle lead to different spectral densities at the Larmor frequency of the carbon, ω_C, for the CSA mechanism and the dipole–dipole mechanism. The close agreement between the solid-state experiment and the liquid state relaxation experiment presented here indicates that, in practice, anisotropic motions are not a problem in our system. In a recent article (Fushman and Cowburn, 1999) it was shown that the difference between the spectral densities for tensors with different orientations in the molecular frame is smaller for the spectral density at the Larmor frequency compared to zero frequency. This indicates that the potential problem of anisotropic motions when estimating the CSA from relaxation rates may be relatively small for longitudinal relaxation, which is dominated by $J(\omega_C)$. This is in contrast to transverse relaxation, which is dominated by $J(0)$. $J(0)$ is in turn very sensitive to anisotropic motion. However, in the general case anisotropic motion will certainly affect the results obtained by both methods. In the present case our preliminary theoretical analysis indicates that in a system with high anisotropy and where $\omega_c\tau_c$ is far from unity (τ_c is

Table 2. Magnitude and orientation factor of chemical shift anisotropy for the ortho carbons of tyrosine

Method	σ_{xx}	σ_{yy}	σ_{zz}	$\Delta\sigma_{eff}$	f_{orient}	Reference
NMR relaxation[a]				153±5	−0.76±0.02	This work
NMR relaxation[b]				156±5	−0.77±0.02	This work
Solid-state NMR	−15.7[c]	51.0[c]	167.1[c]	160.2	−0.78	Frydman et al., 1992
Solid-state NMR	−18.43[c]	45.8[c]	166.4[c]	162.5	−0.77	Frydman et al., 1992
Ab initio	−16.4[d]	75.3[d]	168.4[d]	160.1	−0.79	This work
Ab initio	−23.7[d]	61.9[d]	176.6[d]	174.03	−0.82	This work

[a]Obtained without taking the effect of other protons in the vicinity into account using Equations 4 and 5.
[b]Obtained using Equations 14, 15 and 16 where the effect of other protons is taken into account.
[c]Adapted from Frydman et al. (1992) assuming an absolute isotropic shielding of TMS of 182.5 ppm as obtained using Gaussian98 with the same protocol as for *p*-cresol. The two rows correspond to the two non-equivalent ortho carbons in tyrosine.
[d]From Gaussian98 calculation on *p*-cresol described in the Results section. The double set of data results from the two non-equivalent ortho carbons in *p*-cresol. From the ab initio calculation we could draw the conclusion that the CSA tensor x-axis is parallel to the CH bond, the z-axis is orthogonal to the plane of the ring and the y-axis is orthogonal to the other two. These orientations were assumed when calculating the orientation factors, f_{orient}, from the shielding tensor principal values obtained by solid-state NMR.

the overall rotational correlation time), the systematic error in the parameters caused by anisotropic motion may be significantly increased (P. Damberg, unpublished results).

(2) Another effect that could give rise to systematic errors is the possible interference from relaxation mechanisms other than CSA and dipole–dipole between the heterospin and the attached proton. The effect of other protons in the vicinity of the investigated pair of nuclei has a small but perhaps not negligible contribution to carbon longitudinal relaxation. In order to evaluate this possible effect we assume that the spectral densities at the Larmor frequency of the carbon for the vectors between the carbon and the protons in the vicinity are identical to the spectral density for the vector between the carbon and the attached proton. Further we calculate $k = (\sum_i r_{CH^i}^{-6})/r_{CH}^{-6}$, where i runs over all protons except the one attached to the carbon. From the motilin solution structure (Edmondson et al., 1991) the effect of other protons was calculated to be about 2.5% of the effect of the attached proton, which is more than the experimental error. Since the same effect adds to the autorelaxation of the two-spin order it is straightforward to replace Equation 2 with an equation where the effect of other protons in the vicinity is taken into account. A general way of taking the effect of other protons into account in the frame of the spectral density mapping is given in the appendix.

We obtain:

$$J(\omega_C) = \frac{(1-k)\rho_C + (1+k)(\rho_{CH} - \rho_H)}{2\left(\frac{1}{3}\Delta\sigma_{eff}^2 B_0^2 \gamma_C^2 + 3\left(\frac{\mu_0}{4\pi}\right)^2 \frac{\hbar^2\gamma_H^2\gamma_C^2}{4r_{CH}^6}(1+k)\right)} \tag{13}$$

Equation 3 is replaced by:

$$B_0 \frac{(1-k)\rho_C + (1+k)(\rho_{CH} - \rho_H)}{\delta_C} = slope \cdot B_0^2 + intercept \tag{14}$$

and the effective magnitude, corrected for the effect of other protons in the vicinity, becomes:

$$|\Delta\sigma| = \sqrt{\frac{slope(1+k)}{intercept}} \cdot \frac{3\hbar\gamma_H\mu_0}{8\pi r_{CH}^3} \tag{15}$$

and the orientation factor:

$$|f_{orient}| = |P_2(\cos(\beta))| = \sqrt{\frac{(1+k)}{slope \cdot intercept}} \tag{16}$$

With $k = 0.025$ this means that protons other than the attached one are 2.5% as effective in causing carbon relaxation as the attached proton, the estimated value for the effective CSA magnitude increases

to 156±5 ppm and the orientation factor becomes −0.77±0.02 (Table 2). Those values are slightly higher but within error limits of the values obtained without any attempt to take this effect into account.

Conclusions

The magnitude of the chemical shift anisotropy as well as precise information concerning the orientation of the CSA tensor for a pair of spin 1/2 nuclei can be estimated from only longitudinal relaxation rates at two or more fields, without having to assume any motional model.

Acknowledgements

Britt-Marie Olsson is acknowledged for peptide synthesis. Kalle Kaljuste is acknowledged for help with attaching the t-Boc protecting group on the labeled tyrosine. Kyung-Bin Cho is acknowledged for carrying out the quantum chemical calculations and the Swedish NMR center is acknowledged for the use of their 800 MHz NMR spectrometer.

References

Allard, P., Jarvet, J. and Gräslund, A. (1997) *J. Magn. Reson.*, **124**, 97–103.

Boyd, J., Hommel, U. and Campbell, I.D. (1990) *Chem. Phys. Lett.*, **175**, 477–482.

Boyd, J. and Redfield, C. (1998) *J. Am. Chem. Soc.*, **120**, 9692–9693.

Canet, D. (1998) *Concepts Magn. Reson.*, **10**, 291–297.

Dayie, K.T. and Wagner, G. (1994) *J. Magn. Reson.*, **A111**, 121–126.

Edmondson, S., Khan, N., Shriver, J., Zdunek, J. and Gräslund, A. (1991) *Biochemistry*, **30**, 11271–11279.

Felli, I., Desvaux, H. and Bodenhausen, G. (1998) *J. Biomol. NMR*, **12**, 509–521.

Freeman, R. and Hill, H.D.W. (1971) *J. Chem. Phys.*, **54**, 3367–3377.

Frydman, L., Chingas, G.C., Lee, Y.K., Grandinetti, P.J., Eastman, M.A., Barrall, G.A. and Pines, A. (1992) *Isr. J. Chem.*, **32** ,161–164.

Fushman, D. and Cowburn, D. (1998a) *J. Am. Chem. Soc.*, **120**, 7109–7110.

Fushman, D., Tjandra, N. and Cowburn, D. (1998b) *J. Am. Chem. Soc.*, **120**, 10947–10952.

Fushman, D. and Cowburn, D. (1999) *J. Biomol. NMR*, **13**, 139–147.

Goldman, M. (1984) *J. Magn. Reson.*, **60**, 437–452.

Kay, L., Nicholson, L., Delaglio, F., Bax, A. and Torchia, D. (1992) *J. Magn. Reson.*, **97**, 359–375.

Kroenke, C.D., Loria, J.P., Lee, L.K., Rance, M. and Palmer, A.G. (1998) *J. Am. Chem. Soc.*, **120**, 7905–7915.

Kupče, Ē., Boyd, J. and Campbell, I.D. (1995) *J. Magn. Reson.*, **B106**, 300–303.

Najfeld, I., Kwaku, T., Wagner, G. and Havel, T. (1997) *J. Magn. Reson.*, **124**, 372–382.

Norwood, T.J. (1996) *J. Magn. Reson.*, **A120**, 278–283.

Norwood, T.J. (1997) *J. Magn. Reson.*, **125**, 265–279.

Ottiger, M., Tjandra, N. and Bax, A. (1997) *J. Am. Chem. Soc.*, **119**, 9825–9830.

Palmer, A.G., Rance, M. and Wright, P.E. (1991) *J. Am. Chem. Soc.*, **113**, 4371–4380.

Palmer, A.G., Cavanagh, J., Byrd, R.A. and Rance, M. (1992) *J. Magn. Reson.*, **96**, 416–424.

Peng, J.W. and Wagner, G. (1992) *J. Magn. Reson.*, **98**, 308–332.

Pervushin, K., Riek, R., Wider, G. and Wüthrich, K. (1997) *Proc. Natl. Acad. Sci. USA*, **94**, 12366–12371.

Tessari, M., Mulder, F., Boelens, R. and Vuister, G. (1997a) *J. Magn. Reson.*, **127**, 128–133.

Tessari, M., Vis, H., Boelens, R., Kaptein, R. and Vuister, G.W. (1997b) *J. Am. Chem. Soc.*, **119**, 8985–8990.

Tjandra, N. and Bax, A. (1997a) *J. Am. Chem. Soc.*, **119**, 9576–9577.

Tjandra, N. and Bax, A. (1997b) *J. Am. Chem. Soc.*, **119**, 8076–8082.

Tjandra, N., Szabo, A. and Bax, A. (1996) *J. Am. Chem. Soc.*, **118**, 6986–6991.

Appendix

In this appendix we describe how the small contribution to carbon relaxation from other protons can be taken into account when doing spectral density mapping. It is assumed that the spectral density functions are the same for all vectors between any proton and the carbon under study.

The six relaxation rates used in the spectral density mapping procedure can be expressed as a linear combination of the spectral densities at five frequencies and a constant describing the contribution to longitudinal proton relaxation from other protons. The coefficients are the sum of the coefficients for the relaxation mechanisms, DD, CSA and the contribution from other protons, for each relaxation rate.

$$\overrightarrow{R} = \left(\mathbf{M}^{\mathrm{DD}} + \mathbf{M}^{\mathrm{CSA}} + \mathbf{M}^{\substack{other\\protons}}\right) \cdot \overrightarrow{J} \tag{A1}$$

The spectral densities can be obtained as:

$$\overrightarrow{J} = \left(\mathbf{M}^{\mathrm{DD}} + \mathbf{M}^{\mathrm{CSA}} + \mathbf{M}^{\substack{other\\protons}}\right)^{-1} \cdot \overrightarrow{R}^{\,\mathrm{experimental}} \tag{A2}$$

where

$$\overrightarrow{J} \equiv \begin{pmatrix} J(0) \\ J(\omega_C) \\ J(\omega_H - \omega_C) \\ J(\omega_H) \\ J(\omega_H + \omega_C) \\ \rho_{H^{3,5}H^i} \end{pmatrix} \text{ and } \overrightarrow{R} \equiv \begin{pmatrix} \rho_{\mathrm{C}} \\ \lambda_{\mathrm{C}} \\ \lambda^a_{\mathrm{C}} \\ \rho_{\mathrm{CH}} \\ \rho_{\mathrm{H}} \\ \sigma_{\mathrm{CH}} \end{pmatrix} \tag{A3}$$

ρ_{C} is the autorelaxation rate of longitudinal carbon magnetization, λ_{C} is the autorelaxation rate of transverse carbon magnetization, λ^a_{C} is the autorelaxation rate of transverse antiphase coherence with carbon as the active spin, ρ_{CH} is the autorelaxation rate of longitudinal two-spin order, ρ_{H} is the autorelaxation rate of longitudinal proton magnetization and σ_{CH} is the sum of the carbon proton cross-relaxation rates (dominated by the attached proton) (Allard et al., 1997). The symbol $\rho_{H^{3,5}H^i}$ is the contribution to longitudinal autorelaxation of the proton from other protons in the vicinity.

$$\mathbf{M}^{\mathrm{DD}} = d \begin{pmatrix} 0 & 3 & 1 & 0 & 6 & 0 \\ 2 & \frac{3}{2} & \frac{1}{2} & 3 & 3 & 0 \\ 2 & \frac{3}{2} & \frac{1}{2} & 0 & 3 & 0 \\ 0 & 3 & 0 & 3 & 0 & 0 \\ 0 & 0 & 1 & 3 & 6 & 0 \\ 0 & 0 & -1 & 0 & 6 & 0 \end{pmatrix} \tag{A4}$$

where

$$d = \left(\frac{\mu_0}{4\pi}\right)^2 \frac{\hbar^2 \gamma_{\mathrm{H}}^2 \gamma_{\mathrm{C}}^2}{4 r_{\mathrm{CH}}^6} \tag{A5}$$

and

$$\mathbf{M}^{\mathrm{CSA}} = c \begin{pmatrix} 0 & 3 & 0 & 0 & 0 & 0 \\ \frac{2}{3} & \frac{1}{2} & 0 & 0 & 0 & 0 \\ \frac{2}{3} & \frac{1}{2} & 0 & 0 & 0 & 0 \\ 0 & 3 & 0 & 0 & 0 & 0 \\ 0 & 0 & 0 & 0 & 0 & 0 \\ 0 & 0 & 0 & 0 & 0 & 0 \end{pmatrix} \tag{A6}$$

$$c = \frac{1}{3} \Delta\sigma^2 B_0^2 \gamma_C^2 \tag{A7}$$

and, in analogy with the treatment of the effect of vicinal protons upon proton relaxation by Peng and Wagner (1992):

$$\mathbf{M}^{\substack{other\\protons}} = kd \begin{pmatrix} 0 & 3 & 1 & 0 & 6 & 0 \\ 2 & \frac{3}{2} & \frac{1}{2} & 3 & 3 & 0 \\ 2 & \frac{3}{2} & \frac{1}{2} & 3 & 3 & \frac{1}{kd} \\ 0 & 3 & 1 & 0 & 6 & \frac{1}{kd} \\ 0 & 0 & 0 & 0 & 0 & \frac{1}{kd} \\ 0 & 0 & -1 & 0 & 6 & 0 \end{pmatrix} \tag{A8}$$

where

$$k = \left(\sum_i r_{CH^i}^{-6}\right) / r_{CH}^{-6} \tag{A9}$$

and i runs over all protons except the one attached to the carbon. The matrix formulation of Equation A2 would then become:

$$\begin{pmatrix} J(0) \\ J(\omega_C) \\ J(\omega_C - \omega_H) \\ J(\omega_H) \\ J(\omega_C + \omega_H) \\ \rho_{H^{3,5}H^i} \end{pmatrix} = \begin{pmatrix} -\frac{3(1-k)}{8(c+3d(1+k))} & \frac{3(1-k)}{4(c+3d(1+k))} & \frac{3(1+k)}{4(c+3d(1+k))} & -\frac{3(1+k)}{4(c+3d(1+k))} & \frac{3(1+k)}{8(c+3d(1+k))} & 0 \\ \frac{1-k}{2(c+3d(1+k))} & 0 & 0 & \frac{1+k}{2(c+3d(1+k))} & -\frac{1+k}{2(c+3d(1+k))} & 0 \\ \frac{1}{4d} & 0 & 0 & -\frac{1}{4d} & \frac{1}{4d} & -\frac{1}{2d(1+k)} \\ -\frac{1}{12d} & \frac{1}{6d} & -\frac{1}{6d} & \frac{1}{12d} & \frac{1}{12d} & 0 \\ \frac{1}{24d} & 0 & 0 & -\frac{1}{24d} & \frac{1}{24d} & \frac{1}{12d(1+k)} \\ -\frac{1}{4} & -\frac{1}{2} & \frac{1}{2} & \frac{1}{4} & \frac{1}{4} & 0 \end{pmatrix} \cdot \begin{pmatrix} \rho_{\mathrm{C}} \\ \lambda_{\mathrm{C}} \\ \lambda_{\mathrm{C}}^{a} \\ \rho_{\mathrm{CH}} \\ \rho_{\mathrm{H}} \\ \sigma_{\mathrm{CH}} \end{pmatrix}$$

where the second row corresponds to Equation 13.